

Single domain transport measurements of C₆₀ films

S. Rogge, M. Durkut, and T.M. Klapwijk

Department of Applied Physics and DIMES, Delft University of Technology, Lorentzweg 1, 2628 CJ Delft, The Netherlands

(Dated: 9th November 2018)

Thin films of potassium doped C₆₀, an organic semiconductor, have been grown on silicon. The films were grown in ultra-high vacuum by thermal evaporation of C₆₀ onto oxide-terminated silicon as well as reconstructed Si(111). The substrate termination had a drastic influence on the C₆₀ growth mode which is directly reflected in the electrical properties of the films. Measured on the single domain length scale, these films revealed resistivities comparable to bulk single crystals. *In situ* electrical transport properties were correlated to the morphology of the film determined by scanning tunneling microscopy. The observed excess conductivity above the superconducting transition can be attributed to two-dimensional fluctuations.

In contrast to conventional inorganic semiconductors, the electrical properties of organic semiconductors directly reflect the electronic structure of the molecules they consist of. Due to the weak Van der Waals binding between the molecules tailoring of the electronic properties of a material is possible on the molecular level. Presently, there is a strong interest in high-quality thin films of organic semiconductors due to the realization of electrostatic doping leading to metallic conduction in these materials¹. Intrinsic material properties can be measured by contacting a single grain in a four probe configuration². This field-effect transistor geometry is very powerful since it allows for a continuous change in carrier density over a large range in one sample which, is almost impossible to realize with chemical doping.

The Van der Waals bonded organic crystals are very fragile. The realization of high-quality thin films on a rigid substrate would make it possible to use high resolution lithography and standard processing, treating these materials in a similar fashion as conventional semiconductors. This would open up the opportunity to study the intrinsic properties of these novel materials as well as mesoscopic physics in an unseen range of carrier densities in one sample. As a starting point to study thin films of organic semiconductors we have chosen the well-investigated system K₃C₆₀. The growth as well as the superconducting transition of this material have been studied in detail^{3,4}. The motivation for starting with a chemically instead of an electrostatically doped system is the larger freedom in choosing a substrate. Furthermore, the preparation of an oxide which allows for the high surface charge necessary to achieve superconductivity with field doping is highly nontrivial. Up to now transport studies of C₆₀ films were done on oxides in contrast to the growth studies of highly ordered films on atomically flat substrates³. Here, we combine transport and morphology studies. Both an atomically flat and an oxide substrate are discussed: 7 × 7 reconstructed Si(111) and SiO₂. Finally, for future electrostatic doping of high-quality C₆₀ films it is possible to combine atomically flat surfaces with a gate by using Si on SiO₂⁵.

In this paper we combine *in situ* scanning tunneling microscopy (STM) with transport experiments to link the film morphology to the electrical properties. Fluctu-

ation effects above the superconducting transition were analyzed to further determine the film quality (dimensionality). It was found that the substrate termination has a drastic influence on the electrical properties of the film. On oxide, ultra-thin films show thermally activated transport. On atomically flat reconstructed Si, films remained superconducting down to a thickness of at least 25 monolayers (ML). The resistivity of these films is comparable to what has been reported for the best single crystals.

Film growth, STM analysis, and transport measurements were all carried out in a single ultra-high vacuum (UHV) system with a base pressure of $5 \cdot 10^{-11}$ mbar to prevent K oxidation. Low-doped silicon substrates (50 Ω·cm and 17 kΩ·cm p-type wafers from standard stock) were used to keep the background conduction low. For the films discussed here the parallel conduction through the Si can be neglected below 225 K.

C₆₀ films on two kinds of Si surface termination have been studied, the 7×7 reconstruction on Si(111) and Si oxide which is a common substrate for transport experiments. A native oxide was prepared by oxidizing a hydrogen-passivated Si substrate in nitric acid. After loading into UHV the substrate was degassed at 800 K for several hours. To prepare the 7×7 reconstruction the substrate was further annealed at 1100 K for one hour. The C₆₀ was evaporated onto the room temperature substrate from a Knudsen-cell. Films with thicknesses between 1 and 140 ML were prepared at a growth-rate of about 2 ML/hour. It is necessary to quote mean thickness due to the Stranski-Krastanov growth mode of C₆₀ on Si leading to island formation. The thickness was based on the C₆₀ evaporation time after careful calibration of the source based on STM scans.

Very different growth modes were observed for the two substrate terminations. Figure 1 shows two films of similar thickness, one on the 7×7 reconstruction of Si(111) (a) and the other on SiO₂ (b). The film on reconstructed Si consists of coalesced islands/grains with the (111) surface of the C₆₀ fcc lattice parallel to the substrate as expected for the Stranski-Krastanov growth mode. In contrast, a film of similar thickness on an oxide-terminated surface shows small grains without a common [111] direction. These grains show a much weaker tendency to coalesce

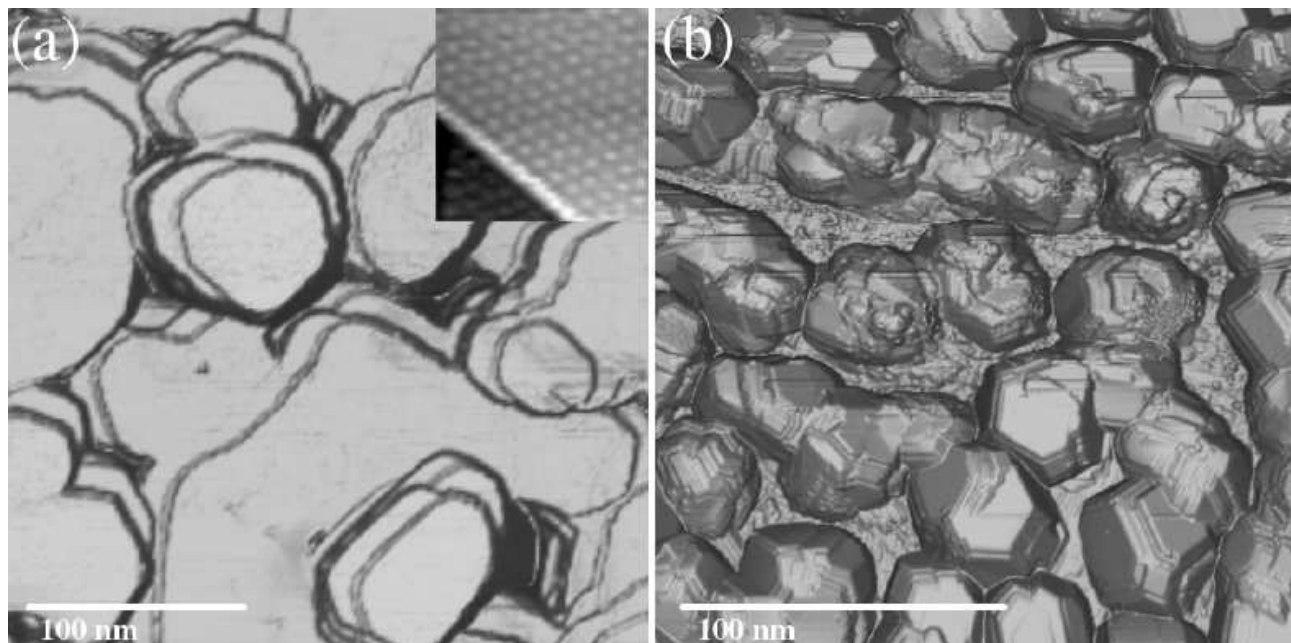


Figure 1: STM scans of K_3C_{60} films on 7×7 terminated Si (a) and oxide terminated Si (b). The images represent a top view onto a pseudo three-dimensional light-shaded surface. The inset shows molecular ordering in (a). On the reconstructed substrate (a) islands/grains coalesce, all with the (111) surface parallel to the substrate (average total thickness 17 nm, height range of scan 12 nm). On oxide (b) the randomly oriented grains are observed (average total thickness 11 nm, height range 20 nm). Note the larger scan size of the well order film (a) compared to (b).

which manifests itself in the 2.5 times larger roughness of the films grown on SiO_2 .

To study the electrical transport properties of the films contacts were evaporated onto the substrate before loading it into UHV. Two different contact arrangements were used to probe conductance at different length scales. In one, further referred to as *macro* contacts, tungsten pads were evaporated onto the substrate by using a shadow-mask with channel lengths between 175 and 600 μm (see top inset in Fig. 2). In the other, further referred to as *sub-micron* contacts, e-beam lithography was used to define four tungsten probes with a separation of 250 nm (see bottom inset in Fig. 2).

The resistance of a K_xC_{60} film goes through a minimum as the doping goes through the optimum value of $x = 3$ ($x = 0$ and $x = 6$ are both insulating with $\rho > 10^5 \Omega\cdot cm$). This makes it possible to follow the doping process by monitoring the resistance. *Optimum doping* (i.e. $x = 3$) is achieved when the derivative of the resistance with respect to time crosses zero. A sufficiently low K deposition-rate was used so that diffusion times in these films could be neglected. This was confirmed by annealing experiments which did not lead to a lower resistivity (discussed later on in this paper).

Our ultra-thin films of optimally doped K_3C_{60} on oxide-terminated Si had a considerably higher resistivity than bulk samples and showed thermally activated transport. The sheet resistance of the film on oxide shown in Fig. 1b was 27 $k\Omega/\square$ at room temperature which corresponds to a mean resistivity of $\rho = 30 m\Omega\cdot cm$. The slope

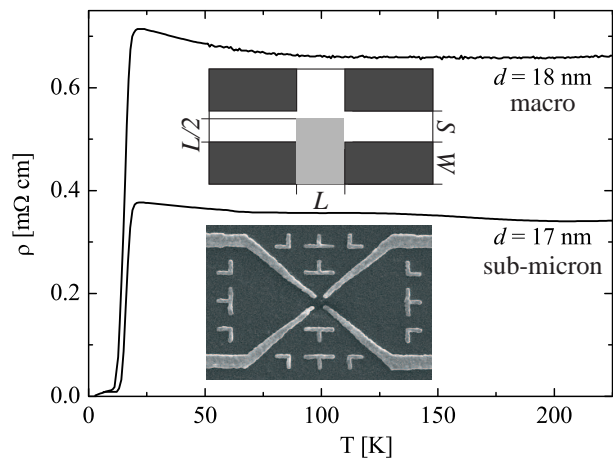


Figure 2: Films on reconstructed Si. The low resistivity trace was measured with the *sub-micron* contacts (250 nm probe separation, scanning electron micrograph in bottom inset). The top trace was measured with the *macro* contacts (top schematic, dark regions represent tungsten pads, channel length $L = 175$ to 600 μm , separation between current and voltage contacts $S = 175 \mu m$, and pad width $W \approx 1000 \mu m$).

of the $\rho(T)$ curve is negative below 300 K as expected for a film with such weakly linked grains. Based on transport experiments Palstra *et al.*⁶ determined a grain size of 7 nm for their films grown on oxide which is consistent with the morphology we observe in Fig. 1b.

Figure 2 shows the resistivities of two films of similar thickness on reconstructed Si measured at two different length scales. In contrast to ultra-thin films on oxide, films of similar thickness on reconstructed Si show a positive ρ vs T slope (metallic behavior) in our measurement between 100 and 300 K. Below 100 K there is a slight rise in resistivity which can be attributed to weak localization in these thin films. The film measured with sub-micron contacts shows the remarkable low resistivity of $0.35 \pm 0.14 \text{ m}\Omega \cdot \text{cm}^{13}$ at 100 K which is at least comparable to the bulk single crystal value of $0.5 \text{ m}\Omega \cdot \text{cm}^7$. Table I lists the detailed parameters of the measurement. The films with the lower resistivity were measured with the sub-micron contact pattern with a probe separation of 250 nm. For the others, the macro pattern with a probe separation of $500 \mu\text{m}$ was used. The factor 2 in resistivity may be understood by looking at the possible origins of disorder and on what length-scale they occur. Grain boundaries are a dominant source of scattering in a doped semiconductor and limit the conductivity especially considering inhomogeneous doping close to the interface. K_3C_{60} is a special material since it has polar surfaces⁸ which could further enhance interface scattering. Our films on reconstructed Si consist of islands with a typical size of 100 to 300 nm (Fig. 1a) which is comparable to the 250 nm probe separation of the sub-micron pattern. Hence, direct electrical transport measurements were done at the single domain length scale and reveal resistivities much closer to theoretical estimates ($0.12 \text{ m}\Omega \cdot \text{cm}$ which are backed by indirect measurements on bulk single crystals $0.18 \text{ m}\Omega \cdot \text{cm}^7$).

length scale	thickness	ρ	$\rho_{\text{upper-bound}}$	R
250 nm	17 nm	$0.35 \text{ m}\Omega \cdot \text{cm}$	$0.49 \text{ m}\Omega \cdot \text{cm}$	$208 \Omega/\square$
$600 \mu\text{m}$	18 nm	$0.70 \text{ m}\Omega \cdot \text{cm}$	$1.15 \text{ m}\Omega \cdot \text{cm}$	$399 \Omega/\square$
bulk (direct)	-	$0.50 \text{ m}\Omega \cdot \text{cm}$	-	-
bulk (indir.)	-	$0.12 \text{ m}\Omega \cdot \text{cm}$	-	-
bulk theory	-	$0.18 \text{ m}\Omega \cdot \text{cm}$	$0.24 \text{ m}\Omega \cdot \text{cm}$	-

Table I: Comparison of single crystal K_3C_{60} properties and our films measured at the sub-micron and macroscopic length scale (upper-bounds based on the two-terminal resistance). Bulk values were taken from Ref. 7 (indirect determination based on fluctuation conductivity).

To study the influence of disorder we measured ρ vs T before and after 20% additional potassium were supplied to an optimally doped film, see Fig. 3a. The extra potassium caused a lower critical temperature and higher resistivity which can be attributed to disorder due to inhomogeneous doping. To ensure that our samples are in thermal equilibrium we did STM scans and measured $\rho(T)$ before and after annealing of a doped film. Figure 3b shows a $\rho(T)$ trace of an optimally doped film before and after annealing at 575 K for 100 minutes. After the anneal no change in morphology was observed in STM scans¹⁴; however, the resistivity increased. Additional doping lowered the resistivity but it remained

higher than before annealing. In contrast to this, reports on thicker films⁸ and bulk samples⁹ show the lowest resistivity and sharpest superconducting transition after annealing and re-doping cycles. The increase in resistivity after annealing may be attributed to the diffusion of contaminants deactivating some of the potassium. We conclude, that our doping rate is slow enough for these ultra-thin films and that annealing is not necessary.

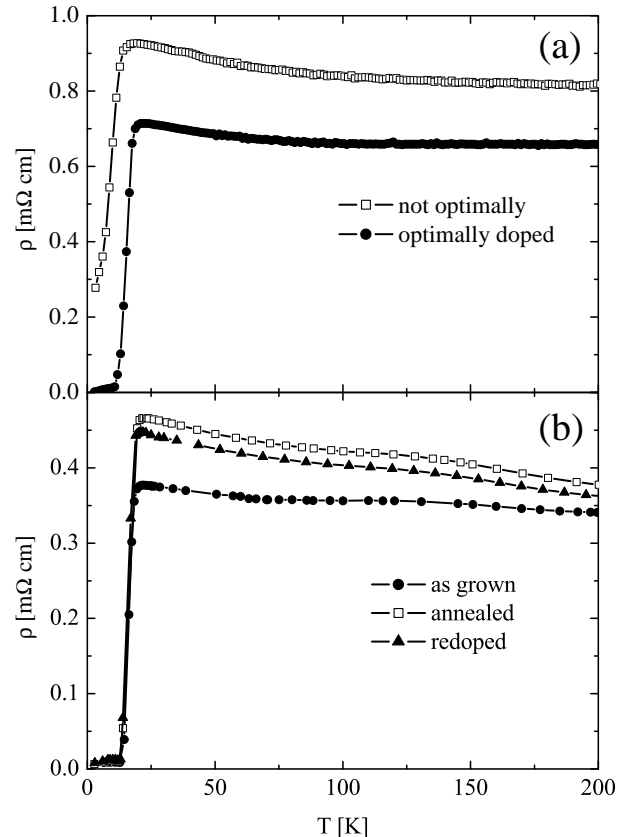


Figure 3: (a) The graph shows two resistivity traces of a K_3C_{60} film, one optimally doped, the other after additional 20% K apparently leading to disorder. (b) This graph shows the negative effect of annealing a film. The first curve is for an optimally doped film; the second (open symbols), after 100 minutes at 575 K; the third, the same film with sufficient additional K to again reach the lowest possible resistance at room temperature.

The superconducting transition of our films is broadened as shown in Fig. 4. This broadening can be attributed to fluctuation effects that lead to an enhanced conductivity above the superconducting transition. The excess conductivity can be described¹⁰ as $\Delta\sigma = \sigma_0 \cdot t^{(d-4)/2}$. Here $t = (T - T_c)/T_c$ is the reduced temperature based on the film transition temperature and d the dimensionality of the film. To find $\Delta\sigma$, the logarithmic contribution to $\rho(T)$ (due to weak localization) was fitted down to 40 K and subtracted from the data. The model for $\Delta\sigma$ with a dimensionality of two yielded a satisfactory fit for the 17 nm ($T_c = 18.5 \text{ K}$) and 18 nm ($T_c = 19 \text{ K}$)

films. As shown in the inset of Fig. 4 we observe the two dimensional fluctuations up to about $t = 0.4$ which notably is above the bulk T_c . A 97 nm thick film could be fit with the three dimensional model ($T_c = 17.5$ K). This is consistent with films which are not dominated by small grains leading to zero dimensional fluctuations independent of film thickness. The length scale is the coherence length. However, this is only a weak indication since magneto-resistance measurements are necessary to conclusively study the two-dimensional effects.

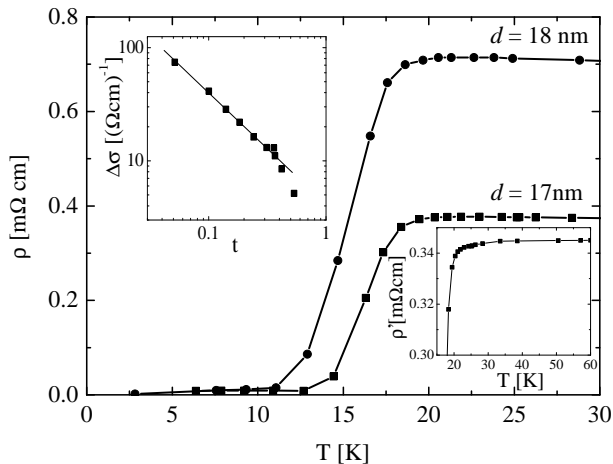


Figure 4: Superconducting transition of the same films as shown in Fig. 2. The insets show the for weak localization corrected $\rho'(T)$ and the excess conductivity $\Delta\sigma$ vs reduced temperature for the 17 nm film including the fit to the two-dimensional fluctuation model.

Hesper *et al.*⁸ reported bulk-like resistivities (0.5 mΩ·cm) of 200 nm thick K_3C_{60} films on aluminum oxide. It seems remarkable that thin films can achieve such good electrical properties. However, due to the Van der Waals bonds of organic semiconductors many of the common problems like surface states and lattice matching to the substrate are not present. Even

so the lattice mismatch between Si and K_3C_{60} is $\approx 250\%$ only the first layer is influenced. The second layer is already perfectly ordered³. Bulk crystals are doped after growth by intercalation⁹ of K causing inhomogenous strain due to the lattice expansion of 0.6%. In these films the strain can be accommodated without creating defects in contrast to bulk samples. Ultra-thin films of organic semiconductors may actually be easier to grow than thicker films since strain and dopant diffusion are less severe problems.

In conclusion, the electrical transport properties of ultra-thin K_3C_{60} films have been evaluated and linked to their morphology. Films grown on reconstructed Si showed resistivities comparable to high-quality single crystals when measured on the single domain length scale. These films remained superconducting down to a mean thickness of at least 17 nm and showed two dimensional excess conductivity due to fluctuations. Similar thin films grown on oxide-terminated silicon had a significantly higher resistivity and showed thermally activated transport without a superconducting transition. The presented results are encouraging in regard to the preparation of thin films of other organic semiconductors since we were able to achieve bulk-like electrical properties by simple thermal evaporation onto a suitable substrate. This technique should be transferable to other molecules that show highly ordered growth on Si, *e.g.* the Phthalocyanines¹¹. The next step is combining well controlled C_{60} films with electrostatic doping since disordered films only yielded resistivities in excess of $10^7 \Omega\cdot\text{cm}$ ¹².

We wish to thank J. Caro and G.D.J. Smit for detailed discussions concerning this work. This work is part of the research program of the "Stichting voor Fundamenteel Onderzoek der Materie (FOM)", which is financially supported by the "Nederlandse Organisatie voor Wetenschappelijk Onderzoek (NWO)". One of us, S.R., wishes to acknowledge fellowship support from the Royal Netherlands Academy of Arts and Sciences.

¹ S. F. Nelson, Y. Y. Lin, D. J. Gundlach, and T. N. Jackson, Appl. Phys. Lett. **72**, 1854 (1998).

² W. A. Schoonveld, J. Vrijmoeth, and T. M. Klapwijk, Appl. Phys. Lett. **73**, 3884 (1998).

³ Y. Z. Li, M. Chander, J. Patrin, J. Weaver, L. P. F. Chibante, and R. Smalley, Science **253**, 429 (1991).

⁴ K. Tanigaki, I. Hirotsawa, T. W. Ebbesen, J. Mizuki, Y. Shimakawa, Y. Kubo, J. S. Tsai, and S. Kuroshima, Nature **356**, 419 (1992).

⁵ M. Noh, G. E. Jellison, F. Namavar, and H. H. Weitering, Appl. Phys. Lett. **76**, 733 (2000).

⁶ T. T. M. Palstra, R. C. Haddon, A. F. Hebard, and J. Zaanen, Phys. Rev. Lett. **68**, 1054 (1992).

⁷ J. G. Hou, V. H. Crespi, X.-D. Xiang, W. A. Vareka, G. Briceno, A. Zettl, and M. L. Cohen, Solid State Comm. **86**, 643 (1993).

⁸ R. Hesper, L. H. Tjeng, A. Heeres, and G. A. Sawatzky,

Phys. Rev. B **62**, 16 046 (2000).

⁹ X.-D. Xiang, J. G. Hou, G. Bracenou, W. A. Bareka, R. Mostovoy, A. Zettl, V. H. Crespi, and M. L. Cohen, Science **256**, 1190 (1992).

¹⁰ W. J. Skocpol and M. Tinkham, Rep. on Prog. in Phys. **38**, 1049 (1975).

¹¹ M. Nakamura, T. Matsunobe, and H. Tokumoto, J. Appl. Phys. **89**, 7860 (2001).

¹² R. C. Haddon, A. S. Perel, R. C. Morris, and A. F. Hebard, Appl. Phys. Lett. **67**, 121 (1995).

¹³ Upper bound is based on two terminal resistance for these thin high-resistive films.

¹⁴ C_{60} starts to desorb from bulk C_{60} at 450 K. However, potassium doping elevates this desorption temperature considerably.